

¹⁷C. M. Lederer, J. M. Jaklevic, and S. G. Prussin, Nucl. Phys. **A135**, 36 (1969).

¹⁸C. M. Lederer, J. M. Hollander, and I. Perlman, *Table of Isotopes* (Wiley, New York, 1967), 6th ed.

¹⁹A. H. Wapstra, in *Proceedings of the Third International Conference on Atomic Masses, Winnipeg, Canada, 1967*, edited by R. C. Barber (Univ. of Manitoba, Winnipeg, Canada, 1967), p. 153.

²⁰F. E. Durham, P. H. Rester, and C. M. Class, in *Proceedings of the International Conference on Nuclear Structure, Kingston, Canada, 1960*, edited by D. A. Bromley and E. W. Vogt (Univ. of Toronto, Toronto, Canada, 1960), p. 594.

²¹G. Alaga, K. Alder, A. Bohr, and B. R. Mottelson, Kgl. Danske Vidensk. Selsk., Mat.-Fys. Medd. **29**, No. 9 (1955).

K^+n CHARGE EXCHANGE AT 12 GeV/c †

A. Firestone, G. Goldhaber, A. Hirata, D. Lissauer, and G. H. Trilling

Department of Physics and Lawrence Radiation Laboratory, University of California, Berkeley, California 94720

(Received 31 July 1970)

We have measured the differential cross section for the reaction $K^+n \rightarrow K^0p$ at 12 GeV/c. We find that (1) the forward amplitude is essentially real, (2) the differential cross section equals that for the reaction $K^-p \rightarrow K^0n$, and (3) the differential cross section agrees well with the predictions of the Regge-pole model of Rarita and Schwarzschild. We have also compiled data on the cross section for the K^+n charge-exchange reaction as a function of incident momentum, and compared it with that for $K^+p \rightarrow K^0\Delta^{++}$. We find that beyond threshold effects these two reactions have the same cross section.

The charge-exchange reaction $K^+n \rightarrow K^0p$ affords the opportunity to study in detail the problems of ρ - A_2 exchange degeneracy, and the validity of the Regge-pole approximation to scattering amplitudes. While this reaction has been studied extensively up to 5.5 GeV/c,¹⁻³ this is the first experiment to report on K^+n charge exchange at a much higher momentum.

The Stanford Linear Accelerator Center 82-in. bubble chamber was exposed to an rf-separated 12-GeV/c K^+ -meson beam. Beam momentum resolution to within $\Delta p/p = \pm 0.2\%$ is achieved by using the known correlation between beam momentum and transverse position in the bubble chamber.⁴ Through the use of a gas Cherenkov counter, pion contamination in the beam is reduced essentially to zero. On the average 8 K^+ mesons were incident in the chamber per pulse. The bubble chamber was filled with deuterium, but there was a hydrogen contamination of 4.5%. Approximately 500 000 exposures were taken, of which about 50% have been analyzed to date.

The film has been scanned for events of the one-prong plus vee and two-prong plus vee topologies. The scanning efficiencies have been determined by an independent rescan on a fraction of the film to be 87% for each topology for a single scan. The events were measured on the Lawrence Radiation Laboratory flying-spot digitizer and were reconstructed and kinematically fitted in the program SIOUX. For those events with invisible spectators (one-prong plus vee), the spec-

tator was assigned a momentum of zero with errors $\Delta p_x = \Delta p_y = \pm 30$ MeV/c, and $\Delta p_z = \pm 40$ MeV/c. All events of each topology which fit the seven-constraint multivertex fit $K^+d \rightarrow K^0pp$, $K^0 - \pi^+\pi^-$, with χ^2 probability greater than 0.1% were accepted as this hypothesis. However, for the events with two visible prongs plus a vee, the spectator is frequently a very short track, and therefore difficult to measure accurately. Although the momentum is adequately determined from range, the angles may be mismeasured for tracks of less than a few millimeters in length. For this reason a five-constraint multivertex fit for the two-prong plus vee events with short recoil, in which the angles of the short recoil are left free, is also performed. Events which fit this special five-constraint hypothesis, but not the seven-constraint hypothesis, are also accepted. There are five such events out of a total of 77 events in the complete sample.

For the reaction $K^+d \rightarrow K^0pp$, 52% of the events have two visible protons and 48% only one visible proton in the bubble chamber. In this final state it is assumed that the slower proton in the laboratory system is the spectator and the faster proton is the recoiling particle. If this choice is made, the slower proton has an observed momentum distribution in agreement with that expected from the Hulthén wave function for momenta less than 300 MeV/c. For the events with $p_{\text{spect}} < 300$ MeV/c, the angular distribution of the spectator in the laboratory system is isotropic. For nine

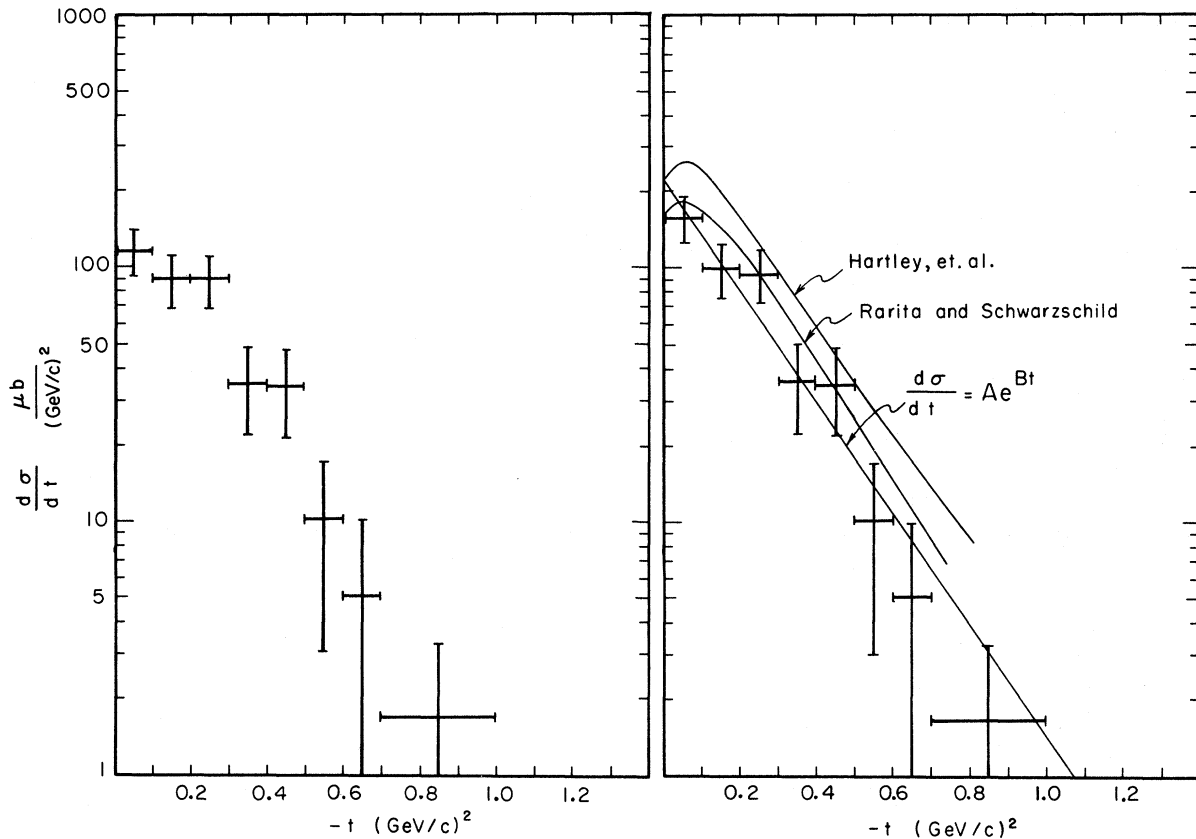


FIG. 1. (a) $d\sigma/dt$ vs t for the reaction $K^+d \rightarrow K^0pp$. (b) $d\sigma/dt$ vs t for the reaction $K^+n \rightarrow K^0p$. The smooth curves are the predictions of models by Hartley *et al.* and by Rarita and Schwarzschild, and the result of a fit by a function of the form $d\sigma/dt = Ae^{Bt}$.

events in the sample (12% of the 77 events) both protons have momenta greater than 300 MeV/c, even though the fraction expected with $p_{\text{spect}} < 300$ MeV/c from the Hulthén wave function is only 1-2%. This difference is generally attributed to double scattering in the deuteron; however, these nine events have been included in the data sample.

Each event has been weighted according to the probability that a K^0 of the observed momentum and production angle decays within the chosen fiducial volume. The cross section has been determined by normalization to the well-known K^+d total cross section at 12 GeV/c,⁵ and has been corrected for the following effects: (1) the topological dependence of scanning efficiencies, (2) measurement efficiencies, (3) hydrogen contamination in the bubble chamber, (4) K^0 escape

probability, and (5) K_2^0 and neutral K_1^0 decays. The cross section for the reaction $K^+d \rightarrow K^0pp$ is $38.7 \pm 4.4 \mu\text{b}$ at 12 GeV/c. The corresponding cross section for the reaction $K^+n \rightarrow K^0p$ is calculated to be $44.5 \pm 5.1 \mu\text{b}$, where corrections for the suppressions due to the Pauli principle in the final state have been made. The calculation of these corrections is described below.

Figure 1(a) shows the measured distribution $d\sigma/dt$ vs t for the reaction $K^+d \rightarrow K^0pp$. Figure 1(b) shows the distribution $d\sigma/dt$ vs t for the charge-exchange reaction $K^+n \rightarrow K^0p$, calculated from the data in Fig. 1(a) by the following method. The differential cross section for the reaction $K^+d \rightarrow K^0pp$ is related to that for the charge-exchange reaction $K^+n \rightarrow K^0p$ by an expression which depends on the deuteron form factor and on the spin-flip and spin-nonflip cross sections. Specifically,

$$\frac{d\sigma}{dt}(K^+d \rightarrow K^0pp) = [1 - S(t)] \left. \frac{d\sigma}{dt} \right|_{\text{nonflip}}^{\text{CEX}} + [1 - \frac{1}{3}S(t)] \left. \frac{d\sigma}{dt} \right|_{\text{spin flip}}^{\text{CEX}}, \quad (1)$$

in which $S(t)$ is the deuteron form factor. For the Hulthén wave function,

$$S(t) = \frac{2\alpha\beta(\alpha + \beta)}{(\beta - \alpha)^2\sqrt{-t}} \left[\tan^{-1} \frac{\sqrt{-t}}{2\alpha} + \tan^{-1} \frac{\sqrt{-t}}{2\beta} - 2 \tan^{-1} \frac{\sqrt{-t}}{\alpha + \beta} \right], \quad (2)$$

in which the values $\alpha = 45.6$ MeV and $\beta = 7\alpha$ have been used. This expression ignores final-state interaction and double-scattering effects. The t dependence of the deuteron form factor is approximately $S(t) \sim \exp(At)$, where $A = 22$ (GeV/c) $^{-2}$.

From Eq. (1) it is clear that in order to apply the deuteron correction properly one must know the relative size of the spin-flip and spin-nonflip cross sections. This ratio is in general unknown except in the forward direction, where the spin-flip cross section must vanish. In the present calculation we have assumed that the spin-flip term is small, and it has been neglected. This deuteron correction is significant only in the region $t < 0.1$ (GeV/c) 2 . A least-squares fit to the data of Fig. 1(b) for a function of the form $d\sigma/dt = Ae^{Bt}$ yields values of $A = 218 \pm 18$ $\mu\text{b}/(\text{GeV}/c)^2$ and $B = 5.0 \pm 0.4$ (GeV/c) $^{-2}$. The χ^2 for this fit is 3.9 for five degrees of freedom.

Figure 1(b) also shows the predictions of models by Rarita and Schwarzschild⁶ and by Hartley et al.⁷ The model of Rarita and Schwarzschild uses ρ , A_2 , and ρ' trajectories, whose parameters have been determined by a fit to a variety of reactions including K^+n charge exchange at the single momentum of 2.3 GeV/c. The curve generated for 12 GeV/c is not a fit, but is a prediction using the identical parameters found at low energy. The agreement is reasonably good. The prediction of Hartley et al. is based on a cut-plus-pole model, but this model predicts too large a cross section for K^+n charge exchange at 12 GeV/c.

In an earlier K^+d experiment at 2.3 GeV/c, Butterworth et al.¹ observed that the K^+n charge-exchange amplitude was dominated by its real part. This has been confirmed at 3 GeV/c by Goldschmidt-Clermont et al.² and also follows from the work of Cline et al.³ In order to determine the relative strengths of the real and imaginary parts of the K^+n charge-exchange amplitude, the forward scattering intensity obtained in this experiment is compared with the forward intensity expected from the imaginary part of the amplitude using the optical theorem. Specifically, the optical theorem and isospin conservation predict for the contribution of the imaginary part of the scattering amplitude to the forward differ-

ential cross section

$$\left. \frac{d\sigma}{dt}(\text{Im}f) \right|_{t=0}^{\text{CEX}} = \frac{1}{16\pi} [\sigma_{\text{tot}}(K^+p) - \sigma_{\text{tot}}(K^+n)]^2. \quad (3)$$

The current best values for the cross sections at 12 GeV/c are⁵

$$\begin{aligned} \sigma_{\text{tot}}(K^+p) &= 17.3 \pm 0.1 \text{ mb}, \\ \sigma_{\text{tot}}(K^+n) &= 17.6 \pm 0.4 \text{ mb}. \end{aligned} \quad (4)$$

The optical theorem thus predicts for K^+n charge exchange at 12 GeV/c

$$\left. \frac{d\sigma}{dt}(\text{Im}f) \right|_{t=0}^{\text{CEX}} = 4.6 \pm 8.2 \text{ } \mu\text{b}/(\text{GeV}/c)^2. \quad (5)$$

In this experiment, however, the extrapolated forward scattering cross section is 218 ± 18 $\mu\text{b}/(\text{GeV}/c)^2$. Thus the observed forward intensity is much larger than that predicted by the optical theorem, which indicates that the amplitude is dominated by its real part, in agreement with the low-energy data. In fact, the K^+N total cross section data are consistent with no imaginary part at all, and, coupled with the charge-exchange data, indicate an upper limit of 6% on the ratio $|\text{Im}f(0)/\text{Re}f(0)|^2$. The calculation of the extrapolated forward cross section for the reaction $K^+n \rightarrow K^0p$ depends on the assumption of no spin-flip amplitude. While this is correct in the forward direction, it may not be strictly correct in a neighborhood about the forward direction. Nevertheless the calculation of this upper limit to the imaginary part of the forward amplitude is not sensitive to large spin-flip terms.

The vanishing of the imaginary part of the K^+n charge-exchange amplitude in the forward direction is supporting evidence for the strong exchange degeneracy of the ρ and A_2 trajectories. As pointed out by Cline et al.,³ a powerful test of ρ - A_2 exchange degeneracy is the equality of the differential cross sections

$$\left. \frac{d\sigma}{dt}(K^+n \rightarrow K^0p) \right|_{t=0} \text{ and } \left. \frac{d\sigma}{dt}(K^-p \rightarrow \bar{K}^0n) \right|_{t=0}. \quad (6)$$

Although a complicated conspiracy between residues and trajectory parameters could result in an accidental equality of the K^+n and K^-p charge-

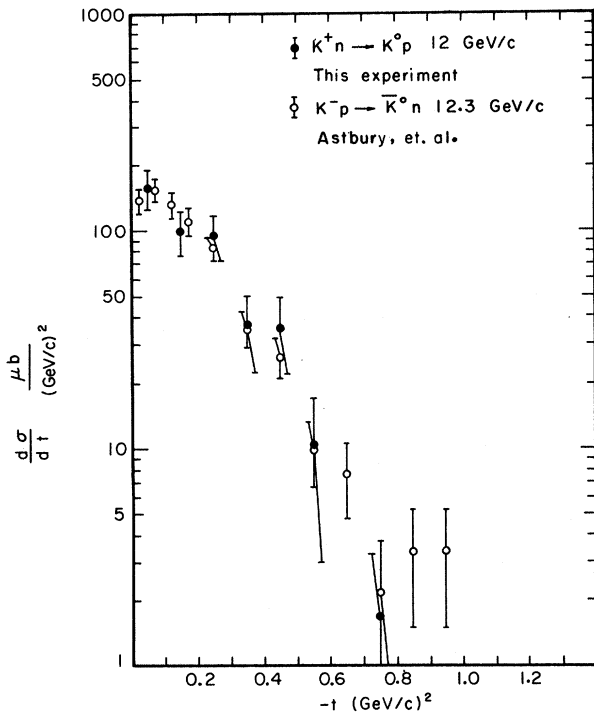


FIG. 2. $d\sigma/dt$ vs t for the charge exchange reactions $K^+n \rightarrow K^0p$ and $K^-p \rightarrow \bar{K}^0n$.

exchange differential cross sections at some values of s and t , this could not be maintained over a wide range of s and t values. Cline *et al.* have shown the equality to be valid for $|t| < 1$ (GeV/c)² at a value of s corresponding to 5.5 GeV/c incident momentum, and Fig. 2 shows the results at 12 GeV/c.⁸ The agreement between K^+ and K^- charge-exchange data at 12 GeV/c is very impressive.

Figure 3(a) shows the cross section for the reaction $K^+d \rightarrow K^0pp$ as a function of incident momentum.⁹ Above 1 GeV/c incident momentum the data can be fitted by a function of the form $\sigma(p) = Ap^{-n}$, where p is the incident momentum. The fit parameters are $A = 7.3 \pm 0.2$ mb and $n = 2.10 \pm 0.05$ with a $\chi^2 = 2.4$ for six data points. For comparison, Fig. 3(b) shows the cross section for the reaction $K^+p \rightarrow K^0\Delta^{++}$,¹⁰ which reaction also involves charge exchange and which is also dominated by ρ and A_2 exchanges. This cross section has also been fitted by a function of the form $\sigma(p) = Ap^{-n}$ for $p \geq 1.96$ GeV/c. The fit parameters are $A = 7.0 \pm 0.2$ mb and $n = 2.00 \pm 0.05$ with a $\chi^2 = 11.2$ for 12 data points. Not only do both cross sections approximately obey a p^{-2} dependence, but both reactions have about the same cross section. Furthermore the shape of $d\sigma/dt$ for both processes is the same within experimental er-

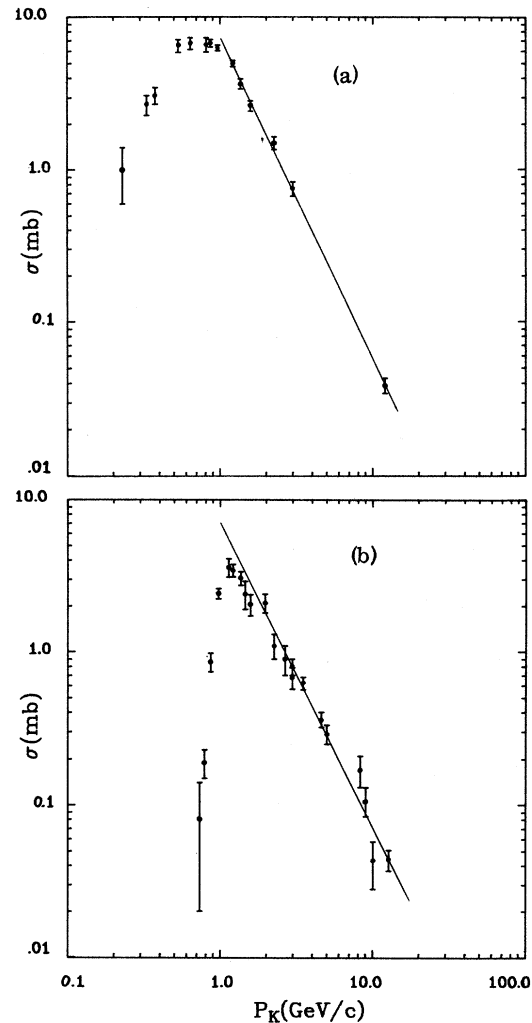


FIG. 3. Cross section versus incident momentum for the reactions (a) $K^+d \rightarrow K^0pp$ and (b) $K^+p \rightarrow K^0\Delta^{++}$.

rors.¹¹ This agreement is remarkable in view of the fact that although the exchanges and the meson vertex are identical for the two reactions, the baryon vertex is different. In the SU(3) classification scheme, the nucleons are members of an octet while the Δ^{++} is a member of a decuplet. Apparently the coupling at a (pnp) or (pnA_2) vertex is approximately equal to that at a $(p\Delta^{++}\rho)$ or $(p\Delta^{++}A_2)$ vertex.

On the other hand, results on the cross section for the reaction $K^-p \rightarrow K^0\Delta^-$, as compiled by Lai and Louie,¹² indicate that from 3 to 5 GeV/c incident momentum this cross section is only about half that for the reaction $K^+p \rightarrow K^0\Delta^{++}$. This is particularly surprising in view of the equality of the K^+n and K^-p charge-exchange differential cross sections at 5 GeV/c.

In conclusion, our study of K^+n charge exchange

at 12 GeV/c indicates (1) agreement with the model of Rarita and Schwarzschild, (2) equality of K^+n and K^-p charge-exchange differential cross sections, and (3) essentially real forward amplitudes for K^+n charge exchange.

We gratefully acknowledge the help of the Stanford Linear Accelerator Center accelerator operation group and in particular we thank J. Murray, R. Gearhart, R. Watt, and the staff of the 82-in. bubble chamber for help with the exposure. We acknowledge the valuable support given by our scanning and programming staff, especially E. R. Burns.

*Work supported by the U. S. Atomic Energy Commission.

¹I. Butterworth *et al.*, Phys. Rev. Lett. **15**, 734 (1965).

²Y. Goldschmidt-Clermont *et al.*, Phys. Lett. **27B**, 602 (1968).

³D. Cline, J. Matos, and D. D. Reeder, Phys. Rev. Lett. **23**, 1318 (1969).

⁴S. Flatté, Lawrence Radiation Laboratory, Berkeley, Group A Memo No. 664 (unpublished).

⁵W. Galbraith *et al.*, Phys. Rev. **138**, B913 (1965).

⁶W. Rarita and B. M. Schwarzschild, Phys. Rev. **162**, 1378 (1968).

⁷B. J. Hartley, R. W. Moore, and K. J. M. Moriarity, Phys. Rev. D **1**, 954 (1970).

⁸P. Astbury *et al.*, Phys. Lett. **23**, 396 (1966).

⁹For incident momenta 0.230, 0.330, 0.377, 0.530, 0.642, and 0.812 GeV/c, see W. Slater *et al.*, Phys. Rev. Lett. **7**, 378 (1961); 0.863, 0.968, 1.211, and 1.364 GeV/c, see A. A. Hirata *et al.*, Phys. Rev. Lett. **21**, 1485 (1968); 1.585 GeV/c, see V. H. Seeger, private communication; 2.260 GeV/c, see Ref. 1; 3 GeV/c, see Ref. 2; and 12 GeV/c, this experiment.

¹⁰For incident momenta 0.735, 0.785, 0.864, 0.969, 1.207, 1.367, and 1.585 GeV/c, see R. Bland *et al.*, Nucl. Phys. **B13**, 595 (1969); 1.140 GeV/c, see E. Boldt *et al.*, Phys. Rev. **133**, B220 (1964); 1.455 GeV/c, see A. Bettini *et al.*, Phys. Lett. **16**, 83 (1965); 1.960 GeV/c, see S. Goldhaber *et al.*, Phys. Rev. **142**, 913 (1966); 2.260 GeV/c, see F. Bomse *et al.*, Phys. Rev. **158**, 1281 (1967); 2.650 GeV/c, see R. Newman *et al.*, Phys. Rev. **158**, 1310 (1967); 2.965 GeV/c, see M. Ferro-Luzzi *et al.*, Nuovo Cimento **39**, 417 (1965); 2.972 GeV/c, see P. Sällström *et al.*, Ark. Fys. **37**, 468 (1968); 3.5, 5.0, and 8.25 GeV/c, see W. De Baere *et al.*, presented to the Fourteenth International Conference on High-Energy Physics, Vienna, 1968 (unpublished); 4.6 GeV/c, see C. Fu, Lawrence Radiation Laboratory Report No. UCRL-18417, 1968 (unpublished); 9 GeV/c, see V. G. Lind *et al.*, Nucl. Phys. **B14**, 1 (1969); 10 GeV/c, see Birmingham-Glasgow-Oxford Collaboration, CERN Report No. 68-7 (unpublished), Vol. II, p. 121; and 12.7 GeV/c; J. C. Berlinghieri *et al.*, Nucl. Phys. **B8**, 333 (1968).

¹¹Berlinghieri, Ref. 10.

¹²K.-W. Lai and J. Louie, Nucl. Phys. **B19**, 205 (1970).

PARTIAL-WAVE ANALYSIS OF THE 3π DECAY OF THE A_2^+

G. Ascoli, D. V. Brockway, H. B. Crawley,* L. B. Eisenstein, R. W. Hanft,† M. L. Ioffredo, and U. E. Kruse

Physics Department, University of Illinois, Urbana, Illinois 61801

(Received 29 June 1970)

A new partial-wave analysis is applied to the 3π decay of the A_2^- in the reaction $\pi^-p \rightarrow p\pi^+\pi^-\pi^-$ at 5 and 7.5 GeV/c. The relative importance of the spins and parities 0^- , 1^+ , 1^- , 2^+ , and 2^- are obtained as a function of 3π mass. Only the 2^+ spin and parity shows resonant structure. Results are also given on the polarization and momentum-transfer dependence of the A_2 and on the mass dependence of the interference of 1^+ background with 2^+ resonance.

Recently there has been renewed interest in the A_2 meson produced in the reaction $\pi^\pm p \rightarrow pA_2^\pm$. At the moment the mass spectra indicate a split peak for π^-p reactions¹ in contrast to a single unsplit peak for the largest π^+ experiment.² To understand this splitting as well as the difference in the π^- and π^+ channels it is very desirable to examine the spin and parity of all decay channels of the A_2 and to understand the production mechanism. The continuing theoretical interest in daughter trajectories also makes it desirable

to look for peaks in other spins and parities in the region of the A_2 mass. The 3π decay mode is particularly useful since the spins and parities 0^- , 1^+ , 2^- , \dots , 1^- , 2^+ , \dots are all allowed whereas for $\eta\pi$ or $K\bar{K}$ decays only 0^+ and 2^+ are expected to be seen.³ In the past,⁴ the experimental information has been limited since most analyses of the 3π final state explored only distributions in the Dalitz plot or only certain angular distributions, and allowed for only one spin and parity above a background. These analyses